

Fits to measurements of rare heavy flavour decays

Ben Allanach^a

^a*DAMTP, University of Cambridge, Wilberforce Road, Cambridge, CB3 0WA, United Kingdom*

E-mail: B.C.Allanach@damtp.cam.ac.uk

ABSTRACT: This write-up is intended to form part of the proceedings for Lepton-Photon 2023. We review the decays $b \rightarrow c\ell\nu_\ell$ (where $\ell \in \{e, \mu, \tau\}$) as well as $b \rightarrow s\mu^+\mu^-$ and $b \rightarrow se^+e^-$, giving the current state of the art in terms of measurements. We review fits to such data of new physics weak effective field theory operators, before closing with simplified interpretations in terms of TeV-scale field theories.

KEYWORDS: Weak interactions, B -anomalies, B hadron decays

Contents

1	$b \rightarrow c\tau\nu$ decays	1
2	$b \rightarrow s\ell^+\ell^-$ processes	3
2.1	Lepton flavour universality ratios	4
3	Weak effective theory fits	4
4	Simple models	8

1 $b \rightarrow c\tau\nu$ decays

Measurements of ratios of the branching ratios

$$R(D^{(*)}) = \frac{B \rightarrow D^{(*)}\tau\bar{\nu}}{B \rightarrow D^{(*)}\ell\bar{\nu}}, \quad (1.1)$$

where $\ell \in \{e, \mu\}$, are of interest because they provide a test of lepton flavour universality (LFU) of the couplings of W^\pm bosons in the Standard Model (SM). A recent estimate of the world average by the HFLAV collaboration put the joint determination of $R(D)$ and $R(D^*)$ at a tension with SM predictions at the 3.2σ level [1]. This tension is called the $b \rightarrow c\tau\nu$ anomaly¹ and has led various authors to suggest that TeV-scale leptoquarks, charged Higgs' or W' particles may be contributing to the process. We show a preliminary 2023 HFLAV combination in Fig. 1, where some measurements have been updated as compared to the preceding official HFLAV combination [2].

Other measurements have recently come to our attention: a 2022 preliminary simultaneous determination of $R(D)$ and $R(D^*)$ from BaBar [3] based on leptonic decays. The previous BaBar determination from 2012 featured in Fig. 1 was based instead on hadronic decays. The 2022 BaBar measurement is reported as

$$R(D) = 0.316 \pm 0.062 \pm 0.019, \quad R(D^*) = 0.226 \pm 0.022 \pm 0.012, \quad \rho = -0.82. \quad (1.2)$$

It is our purpose here to augment the world average by these measurements. We shall perform a more approximate job than has HFLAV. In particular, we have not correlated any systematic errors; otherwise we have added all errors in quadrature. Correlations between R_D and $R(D^*)$ were taken into account, though. To check the level of agreement we obtain with HFLAV's more accurate calculation, we present the results of ours, based on the same data, in Fig. 2. We display 68% confidence level contours consistently throughout (except

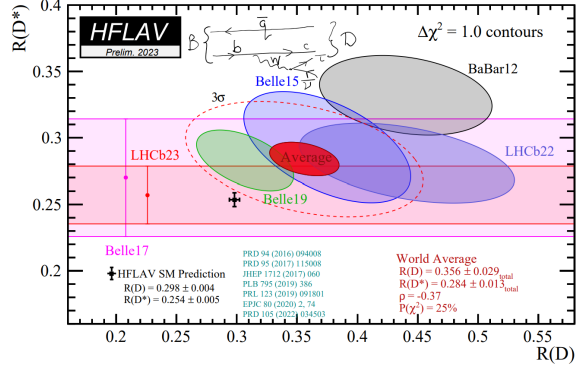


Figure 1: Preliminary HFLAV 2023 world average of $R(D)$ and $R(D^*)$, along with the HFLAV SM predictions. The horizontal bands are 68% confidence level bands, whereas the filled ellipses are 61% bands. The dashed ellipse shows the locus of p -value where a univariate Gaussian distribution would be at 3σ from the maximum. The 61% confidence level (CL) world average is shown as the filled red ellipse. Near the top of the figure, an example leading order Feynman diagram has been sketched in order to show a leading SM contribution to $B \rightarrow D\tau\nu$ decay.

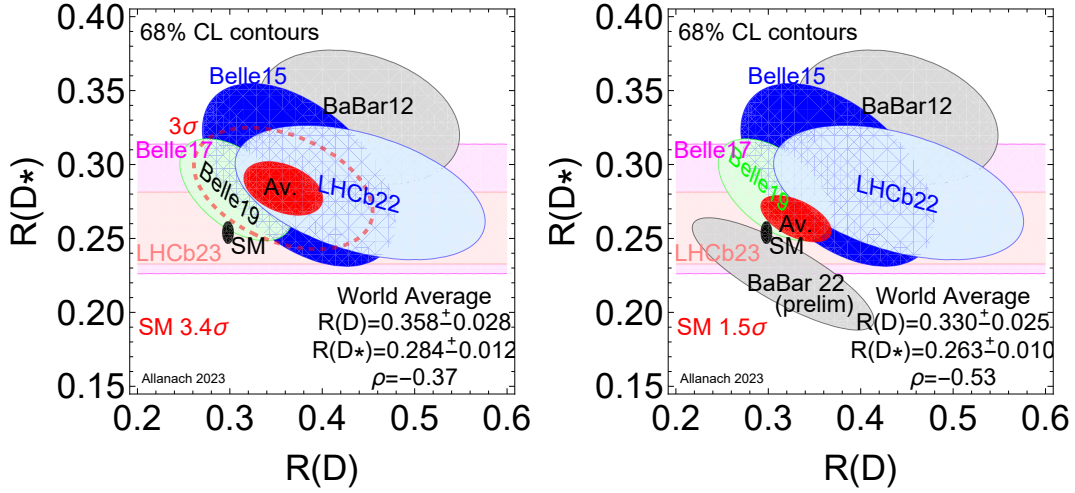


Figure 2: Our determination of the world average of $R(D)$ and $R(D^*)$ and the SM prediction (left panel) excluding and (right panel) including the BaBar 2022 preliminary measurements. The horizontal bands and error ellipses are 68% confidence level bands, except for the dashed ellipse; this shows the locus of iso- p -value where a univariate Gaussian distribution would be at 3σ from the maximum.

for the 3σ one). The results are in fact similar (although one should note the differences

¹We note that each observable implicitly includes an average over different charge decays.

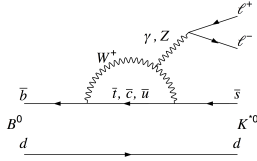


Figure 3: An example of a penguin diagram contributing to the $\bar{B} \rightarrow \bar{K}^{*0} \ell^+ \ell^-$ process.

in appearance coming from choosing somewhat different confidence levels and aspect ratio), showing small differences due to the further approximations of the latter combination. The central values differ by a percent relative error between the two determinations. HFLAV’s determination holds that the tension between data and the SM is at an equivalent univariate Gaussian distribution value (EUGDV) of 3.2σ , whereas our calculation yields 3.4σ . We obtain a p -value of consistency of the measurements is .26 rather than .25. These results are close enough to validate our approximations. Our determination of the world average is

$$R(D) = 0.339 \pm 0.025, \quad R(D^*) = 0.263 \pm 0.01, \quad \rho = -0.53, \quad (1.3)$$

which we calculate to be in only 1.5σ EUGDV tension with the HFLAV 2023 SM prediction. We note here that the preliminary BaBar result is in some tension with the other measurements, reducing the p -value of the data down to an EUGDV of 2.7σ deviation. The calculations used to produce Fig. 2 are included in the ancillary information of the arXiv version of this manuscript. To the best of our knowledge, this is the first time a world average including the 2022 BaBar measurements has appeared in the literature.

Since the combined world average no longer calls strongly for new physics effects in $b \rightarrow c\tau\nu$ decays (although we note the remaining tensions between measurements and that there is still some room for new physics effects), we move on to $b \rightarrow s\ell^+\ell^-$ decays.

2 $b \rightarrow s\ell^+\ell^-$ processes

In the SM, the dominant diagrams contributing to $B \rightarrow K^*\ell^+\ell^-$ are one-loop electroweak box or penguin contributions, such as the penguin contribution shown in Fig. 3. These decays are also useful for testing LFU. The amplitude is suppressed by the loop, by the fact that it is an electroweak process rather than a strong process, and by small CKM angles. This has the result that the branching ratio for $BR(B \rightarrow K^{(*)}\ell^+\ell^-)$ is of order 10^{-6} or less. Since the electron- and muon- masses are much smaller than the B meson mass, they are approximately both massless. This approximation leads to the prediction $BR(B \rightarrow K^{(*)}\mu^+\mu^-) = BR(B \rightarrow K^{(*)}e^+e^-)$, which holds to high precision except at low $q^2 := m_{ll}^2$.

In practice, Feynman diagrams such as the one in Fig. 3 receive QCD corrections. These can be parameterised by form factors (scalar functions of q^2). The predictions for the rare decay $B \rightarrow M\ell^+\ell^-$ then are written in terms of form factors multiplied by kinematic variables and pre-factors. The form factors come in two categories: *local* and *non-local* form factors.

For the local form factors, one can interpolate lattice results which are valid at high q^2 (and therefore low M recoil) and light cone sum rule at low q^2 . The non-local form factors currently have no precise lattice estimates. Several of the SM predictions that are used to produce fits that we shall show use QCD factorisation plus an ad-hoc parameterisation of the long distance contribution which is fit to data (the dominant contribution comes from charm loops). We will also show several SM predictions from the EOS [4, 5] approach. Here, the light cone operator product expansion at $q^2 < 0$ is interpolated/extrapolated to various measurements of branching ratios and angular distributions in decays, which are made at a q^2 value of the J/ψ resonance mass squared, $M_{J/\psi}^2$. Dispersion relations bound the coefficients of a polynomial expansion in terms of a specific kinematic variable, allowing truncations to finite order and a resulting fit of them to a finite number of measurements. In the EOS approach [4, 5], the dominant remaining uncertainty on the relevant predictions typically comes from uncertainties in the local form factors.

The form factors for the SM prediction of $BR(B_s \rightarrow \mu^+\mu^-)$ are known accurately by the lattice, aided by the leptonic final state. We display this branching ratio, jointly measured with $BR(B_s \rightarrow \mu^+\mu^-)$ in Fig. 4, along with some other $b \rightarrow s\mu^+\mu^-$ observables. Fig. 4 shows that several of the observables involving the $b\bar{s}\mu^+\mu^-$ vertex display tensions between SM predictions and measurements, often in several bins of q^2 . We see varying degrees of tension in the SM predictions and data in each observable, although in the CP -untagged $\overline{BR}(B_s \rightarrow \mu^+\mu^-)$ decay, the tension is only mild at 1.6σ of an EUGDV. In the lower two plots, the ordinates have been divided by $BR(B_s \rightarrow KJ/\psi)$ in order to cancel the leading-order dependence upon V_{cb} . Many authors have interpreted the tensions, the ‘ $b \rightarrow s\mu\mu$ anomalies’, as requiring contributions from processes involving quantum fields beyond the SM.

2.1 Lepton flavour universality ratios

LHCb has published a reanalysis [8] of the measurements of R_K and R_{K^*} , where

$$R_X(q^2) = \frac{\int_{q_{min}^2}^{q_{max}^2} BR(B \rightarrow X\mu^+\mu^-(q^2))}{\int_{q_{min}^2}^{q_{max}^2} BR(B \rightarrow Xe^+e^-(q^2))}. \quad (2.1)$$

q_{min}^2 and q_{max}^2 are the two extreme values of q^2 in the particular q^2 bin under consideration. ‘low- q^2 ’ corresponds to $q^2 \in (0.1, 1.1)$ GeV² whereas ‘central- q^2 ’ corresponds to $q^2 \in (1.1, 6.0)$ GeV². These measurements show no significant deviation from the SM. This is a relatively new development, and indicates that, if there is new physics in $b \rightarrow s\mu\mu$ transitions, as indicated above, there may also be associated new physics in $b \rightarrow se^+e^-$ in order that R_K and R_{K^*} may be close to the lepton universality limit.

3 Weak effective theory fits

We now interpret the new physics effects in terms of the Weak Effective Theory (WET), which parameterises the effects of integrated out heavy new physics fields in terms of new

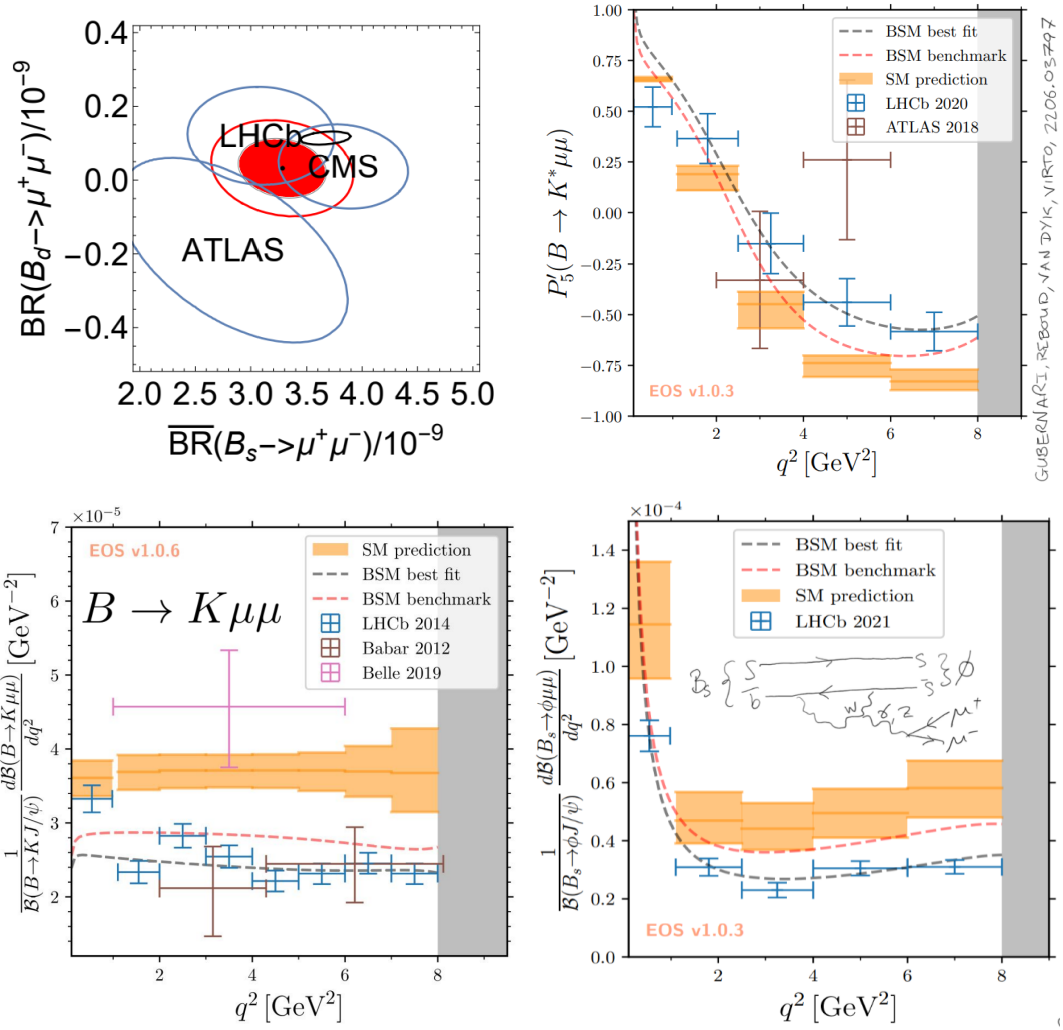


Figure 4: Various SM predictions and measurements of $bs\mu\mu$ processes. (top left) $BR(B_s \rightarrow \mu^+ \mu^-)$: the SM prediction is from Ref. [6] and the combination of data in red is from Ref. [7]. Empty ellipses show the 95% CL constraint in each case. (top right) shows a certain angular distribution variable, P_5' , in $B \rightarrow K^* \mu^+ \mu^-$ decays. (bottom left) shows $BR(B_s \rightarrow \phi \mu^+ \mu^-)$ as a function of q^2 and (bottom right) shows $BR(B \rightarrow K \mu^+ \mu^-)$ decay along with a hand-drawn leading order SM contribution. In the latter three sub-plots, SM predictions are made by EOS [4, 5].

effectively non-renormalisable operators at the weak scale or below. Two such operators that have been shown to be substantially ameliorate the fit to the $b \rightarrow s \mu^+ \mu^-$ anomalies are

$$\mathcal{L} = \dots + N (C_{9\mu}^{NP} (\bar{b} \gamma^\alpha P_L s) (\bar{\mu} \gamma_\alpha \mu) + C_{10\mu}^{NP} (\bar{b} \gamma^\alpha P_L s) (\bar{\mu} \gamma_\alpha \gamma_5 \mu) + H.c.), \quad (3.1)$$

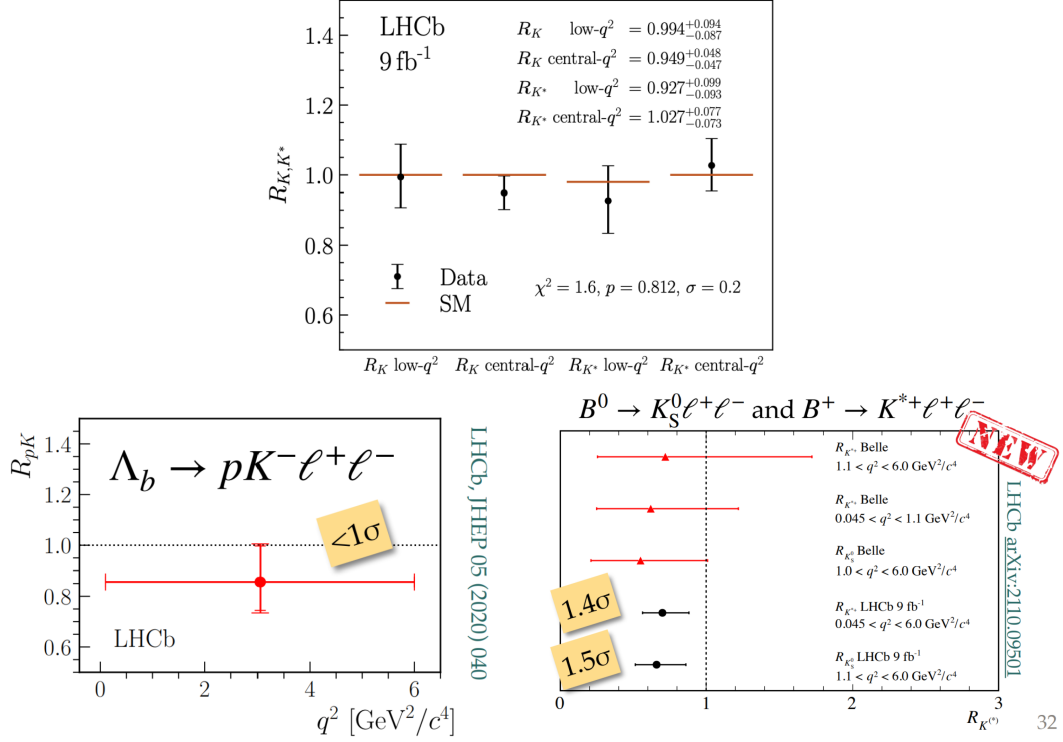


Figure 5: (top) Recent LHCb measurements of R_K and R_{K^*} [8]. (bottom-left) LHCb measurement of R_{pK} . (bottom-right) Belle measurements of R_K and R_{K^*} and LHCb measurements of other LFU ratios.

$N := 4G_F e^2 |V_{ts}| / (16\pi^2 \sqrt{2})$ is a normalising constant, where G_F is the Fermi decay constant, e the electromagnetic gauge coupling and V_{ij} the entries of the CKM matrix. We see the fit by the `flavio` program in the left-hand panel of Fig. 6. Since the three coloured regions overlap at 95% CL, we conclude that there is still some compatibility with the measured values of R_K and R_{K^*} , albeit not perfect because the 68% CL regions do not overlap. The figure also shows a comparison of the fits obtained by different fitting groups in order to show the spread in predictions. While there is broad agreement that the fits disagree with SM predictions², there are some quantitative differences visible between the fits.

Now, we consider also turning on a new physics operator involving di-electron pairs

$$\mathcal{L} = \dots + NC_{9e}^{NP} (\bar{b}\gamma^\alpha P_L s) (\bar{e}\gamma_\alpha e) + H.c. \quad (3.2)$$

We display a joint WET fit to non-zero $C_{9\mu}^{NP}$ and C_{9e}^{NP} in Fig. 7, where we see the preference

²Some estimates in Ref. [11] fit an unidentified non-perturbative SM contribution (that mimics a q^2 -dependent lepton-family universal C_9) in tandem with the new physics WET operators. As argued in Ref. [14], a similar non-perturbative effect cannot explain the 2σ deficit in the $BR(B \rightarrow X_s \mu^+ \mu^-)$ high q^2 -bin, which is compatible with the low q^2 -deficits.

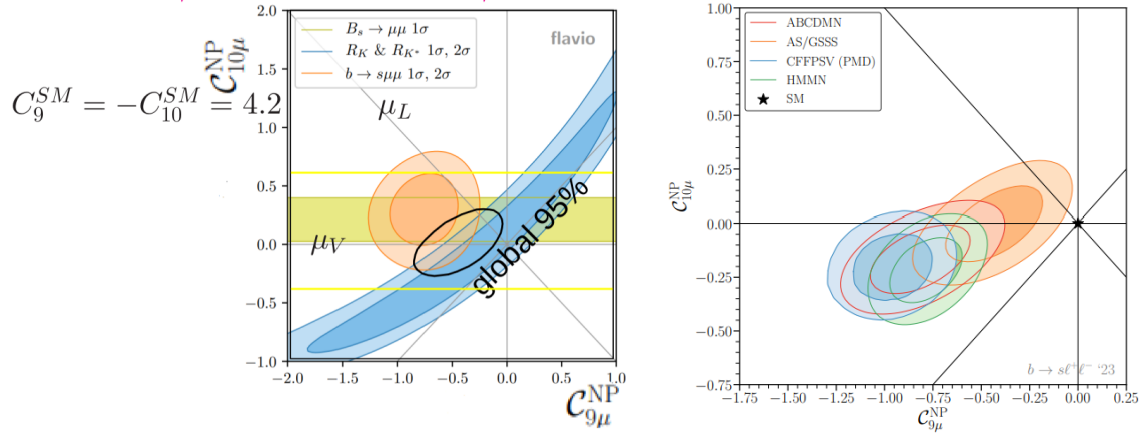


Figure 6: Fits of two non-zero WET operators to $b \rightarrow sll$ anomaly data. The inner (outer) coloured bands show the 68% (95% CL) regions. (left) *flavio* fits [9]. ‘ $b \rightarrow s\mu\mu$ ’ contains observables such as branching ratios and angular distributions etc. The global constraint using all three sets of observables is shown in black at the 95% CL. (right-panel) shows the global fit regions of *flavio* [9] and other fitting groups [10, 11] such as *superIso* [12] which use different sets of experimental data and different treatments of the SM predictions and theoretical uncertainties [13].

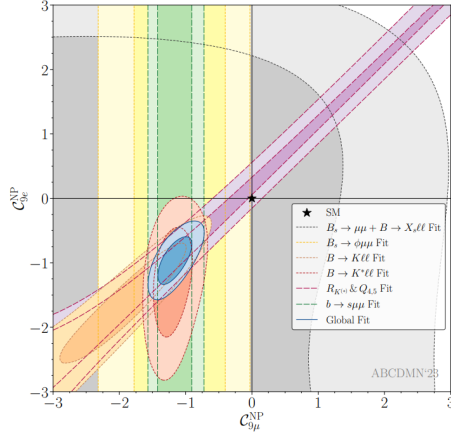


Figure 7: Fits of $C_{9\mu}^{NP}$ and C_{9e}^{NP} to $b \rightarrow sll$ anomaly data. The inner (outer) coloured bands show the 68% (95% CL) regions, respectively. Figure taken from Ref. [10].

for $C_{9e}^{NP} \neq 0$. Overall, the fit has a pull away from the SM limit (the origin), equivalent to a UEDGV of 5.2σ , a significant change for only two fitted parameters.

We now turn to some simple bottom-up models which can generate the non-zero WET operators which we mention above and which were found to significantly ameliorate SM

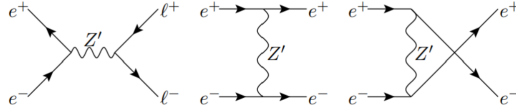


Figure 8: Leading Feynman diagrams of Z' contributions to di-lepton production at the LEP collider.

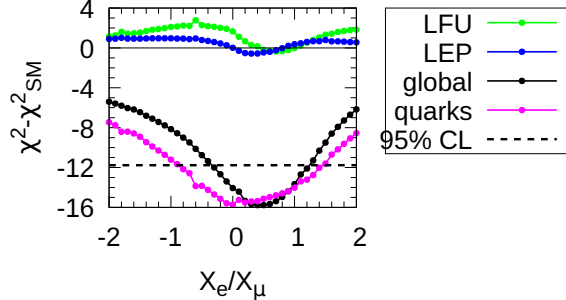


Figure 9: Two parameter fits of a set of Z' models to $b \rightarrow s\ell\ell$ anomaly data. Figure taken from Ref. [15]. Regions below the dashed line are compatible with data globally, to 95% CL, assuming the hypothesis of the line of models.

predictions.

4 Simple models

We examine simple Z' models with a spontaneously broken $U(1)_X$ gauge extension of the SM [15], where

$$3B_3 - (X_e L_e + X_\mu L_\mu + [3 - X_e - X_\mu] L_\tau), \quad (4.1)$$

i.e. where B_3 is third family baryon number, L_e is electron number, L_μ is muon number and X_e and X_τ are arbitrary integer parameters. Such an assignment is anomaly free if electron, muon and tau right-handed neutrinos augment the SM chiral fermion content. Once the Z' is coupled to di-electron pairs as would be implied by $X_e \neq 0$, one should apply bounds from LEP which come from differential measurements of scattering to di-lepton pairs. These do not show significant tensions with SM predictions [16] and so they bound the contributions coming from Feynman diagrams such as those shown in Fig. 8. (??) allows one to interpolate between Z' models which couple to charged leptons via muons only, to those which couple equally to electrons and muons, and even to extrapolate outside of these limits. We display a set of global fits to different values of X_e , for $X_\mu = 10$, in Fig. 9. The figure shows that a significant improvement on χ^2 is obtained as compared to the SM for $X_e/X_\mu \approx 1/2$, although

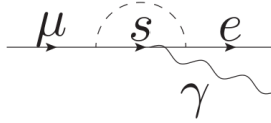


Figure 10: A scalar LQ (that has been fit to $b \rightarrow s\ell^+\ell^-$ anomalies and therefore has a coupling to the strange quark; there is another contribution with $s \rightarrow b$.) contribution to $\mu \rightarrow e\gamma$.

any value in the range $(-0.4, 1.3)$ is within the 95% CL. We also see that the limits of zero coupling of the Z' boson to di-electron pairs and equal coupling to di-electron and di-muon pairs are fit more-or-less equally well, with only a non-significant difference in χ^2 value of 0.7 between them.

We anticipate that requiring a leptoquark (LQ) to couple to electrons and muons with a similar strength in order to fit R_K and R_{K^*} will generically lead to contravention of the $BR(\mu \rightarrow e\gamma) < 4.2 \times 10^{-13}$ (90% CL) bound from the MEG collaboration [17] through processes such as the one shown in Fig. 10. However, Ref. [7] found that LQs that do *not* couple to di-electron pairs, can provide a similar improvement to SM predictions as the ‘ $B_3 - L_2$ ’ model with $X_\mu = 3, X_e = 0$.

Acknowledgements

This work has been partially supported by STFC HEP Theory Consolidated grant ST/000694. We thank other members of the Cambridge Pheno Working group for helpful discussions and Lepton-Photon 2023 for facilitating the talk.

References

- [1] **Heavy Flavor Averaging Group, HFLAV** Collaboration, Y. S. Amhis *et. al.*, *Preliminary average of $r(d)$ and $r(d^*)$ for winter 2023*, .
https://hflav-eos.web.cern.ch/hflav-eos/semi/winter23_prel/html/RDsDsstar/RDRDs.html.
- [2] **Heavy Flavor Averaging Group, HFLAV** Collaboration, Y. S. Amhis *et. al.*, *Averages of b -hadron, c -hadron, and τ -lepton properties as of 2021*, *Phys. Rev. D* **107** (2023), no. 5 052008 [2206.07501].
- [3] Y. Li, *Search for Beyond Standard Model Physics at Babar*. PhD thesis, Caltech, 2022.
<https://resolver.caltech.edu/CaltechTHESIS:05232022-144829107>.
- [4] N. Gubernari, M. Reboud, D. van Dyk and J. Virto, *Improved theory predictions and global analysis of exclusive $b \rightarrow s\mu^+\mu^-$ processes*, *JHEP* **09** (2022) 133 [2206.03797].
- [5] N. Gubernari, M. Reboud, D. van Dyk and J. Virto, *Dispersive Analysis of $B \rightarrow K^{(*)}$ and $B_s \rightarrow \phi$ Form Factors*, 2305.06301.

- [6] T. Feldmann, N. Gubernari, T. Huber and N. Seitz, *Contribution of the electromagnetic dipole operator O_7 to the $B^- s \rightarrow \mu^+ \mu^-$ decay amplitude*, *Phys. Rev. D* **107** (2023), no. 1 013007 [[2211.04209](#)].
- [7] B. Allanach and J. Davighi, *The Rumble in the Meson: a leptoquark versus a Z' to fit $b \rightarrow s \mu^+ \mu^-$ anomalies including 2022 LHCb $R_{K^{(*)}}$ measurements*, *JHEP* **04** (2023) 033 [[2211.11766](#)].
- [8] **LHCb** Collaboration, *Test of lepton universality in $b \rightarrow s \ell^+ \ell^-$ decays*, [2212.09152](#).
- [9] A. Greljo, J. Salko, A. Smolkovič and P. Stangl, *Rare b decays meet high-mass Drell-Yan*, *JHEP* **05** (2023) 087 [[2212.10497](#)].
- [10] M. Algueró, A. Biswas, B. Capdevila, S. Descotes-Genon, J. Matias and M. Novoa-Brunet, *To $(b)e$ or not to $(b)e$: No electrons at LHCb*, [2304.07330](#).
- [11] M. Ciuchini, M. Fedele, E. Franco, A. Paul, L. Silvestrini and M. Valli, *Constraints on lepton universality violation from rare B decays*, *Phys. Rev. D* **107** (2023), no. 5 055036 [[2212.10516](#)].
- [12] F. Mahmoudi, *SuperIso v2.3: A Program for calculating flavor physics observables in Supersymmetry*, *Comput. Phys. Commun.* **180** (2009) 1579–1613 [[0808.3144](#)].
- [13] B. Capdevila, *talk at beyond the flavour anomalies workshop, 2023*, .
- [14] G. Isidori, Z. Polonsky and A. Tinari, *Semi-inclusive $b \rightarrow s \bar{\ell} \ell$ transitions at high q^2* , [2305.03076](#).
- [15] B. Allanach and A. Mullin, *Plan B: New Z' models for $b \rightarrow s l^+ l^-$ anomalies*, [2306.08669](#).
- [16] A. Falkowski and K. Mimouni, *Model independent constraints on four-lepton operators*, *JHEP* **02** (2016) 086 [[1511.07434](#)].
- [17] **MEG** Collaboration, A. M. Baldini *et. al.*, *Search for the lepton flavour violating decay $\mu^+ \rightarrow e^+ \gamma$ with the full dataset of the MEG experiment*, *Eur. Phys. J. C* **76** (2016), no. 8 434 [[1605.05081](#)].